Macromolecules

pubs.acs.org/Macromolecules Article

# Robust and Direct Route for the Development of Elastomeric Benzoxazine Resins by Copolymerization with Amines

Hugo Puozzo,* Shamil Saiev, Leïla Bonnaud, Julien De Winter, Roberto Lazzaroni, and David Beljonne*

Cite This: *Macromolecules* 2022, 55, 10831−10841 Read Online

ACCESS | Metrics & More | Article Recommendations | Supporting Information

**ABSTRACT:** The development of soft pressure sensors, in particular electronic skin, is fundamental to the interfacing between the human body and the outside world, namely, in prosthetics and biomedical applications. In this context, hybrid composite materials incorporating electrically conducting 2D flakes in an insulating matrix show attractive tunable piezoresistive properties suitable for wide-range pressure sensing applications. Here, we report on the design of novel trifunctional benzoxazine precursors for this polymer matrix based on tris(3-aminopropyl)amine and phenol reagents. These precursors have been successfully synthesized and copolymerized with polyetheramines of different lengths to tune the thermomechanical properties of the resulting networks. Extensive molecular dynamics simulations unambiguously relate the changes in glass transition temperature with chemical composition to the variations in the cross-link density and provide $T_g$ values in excellent agreement with the experimental data. With the longest polyetheramine (2000 g mol$^{-1}$), we achieve the synthesis of an elastomeric benzoxazine exhibiting remarkably low $T_g$ of −41 °C, a modulus in compression of 50 kPa, and a shear strain modulus of 300 Pa, with high potential for low-pressure sensing applications.

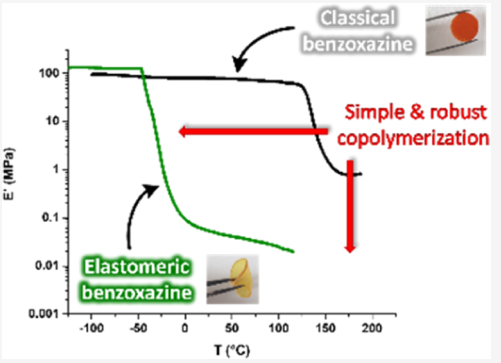




## 1. INTRODUCTION

Polybenzoxazines are an important class of phenolic materials popularized by Ning and Ishida in the nineties.[1] They are attracting much attention and interest from both academic and industrial research groups because they simultaneously combine the easy handling and processing of epoxy resins with the high thermal resistance of bismaleimide and phenolic resins.[2,3] They also show (i) near-zero shrinkage upon curing, (ii) low water absorption, (iii) good thermal and electrical features, and (iv) high char yield.[4−7] In addition, their polymerization can be directly activated thermally without the need of any catalyst. This unique combination of features makes benzoxazine monomers very interesting building blocks in the field of high-performance polymers. Due to their aromatic core, most of the research and development efforts have focused originally on the design of structures to generate networks with a high modulus and a high glass transition temperature.[8−11]

Interestingly, the advantages of benzoxazine resins lie not only in their properties but also in their synthetic accessibility and in the versatility of the reactivity of the benzoxazine functions. Benzoxazine monomers can be prepared following different routes, the most common and easiest way being probably the synthesis by one-pot Mannich condensation of a phenol, a primary amine, and formaldehyde in 1:1:2 molar ratio.[12] This approach allows straight and robust conditions with high yields and limited purification steps. It can be carried out either in bulk or in solvent. As there are many commercially available phenol and amine reagents, benzoxazine monomers are also endowed with a rich flexibility in molecular design.[3,13]

Another important advantage of benzoxazine chemistry is that it is compatible with several other chemistries. In other words, benzoxazine rings are reactive toward other functional groups. This opens the way to the tuning of the curing of benzoxazine precursors by adding a second, reactive component that will participate to/induce the ring-opening addition reaction,[14] similar to the use of hardeners to cure epoxy systems. A number of compounds have already been reported to open the benzoxazine heterocycle and form a new chemical linkage,[13,14] such as thiols, phenolics, chitosan, ammonium, benzimidazoles, and benzoxazoles. In particular, Ishida et al.[15] reported this type of reaction for benzoxazine ring with amines. They showed that primary amines attached to a benzoxazine monomer can enhance its reactivity. Endo et al.[14] demonstrated more recently the copolymerization of amines and benzoxazines via ring-opening addition and revealed the more complex mechanism of this system when

Received: August 1, 2022
Revised: November 14, 2022
Published: December 5, 2022

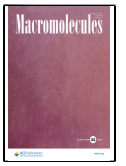





https://doi.org/10.1021/acs.macromol.2c01593
*Macromolecules* 2022, 55, 10831−10841

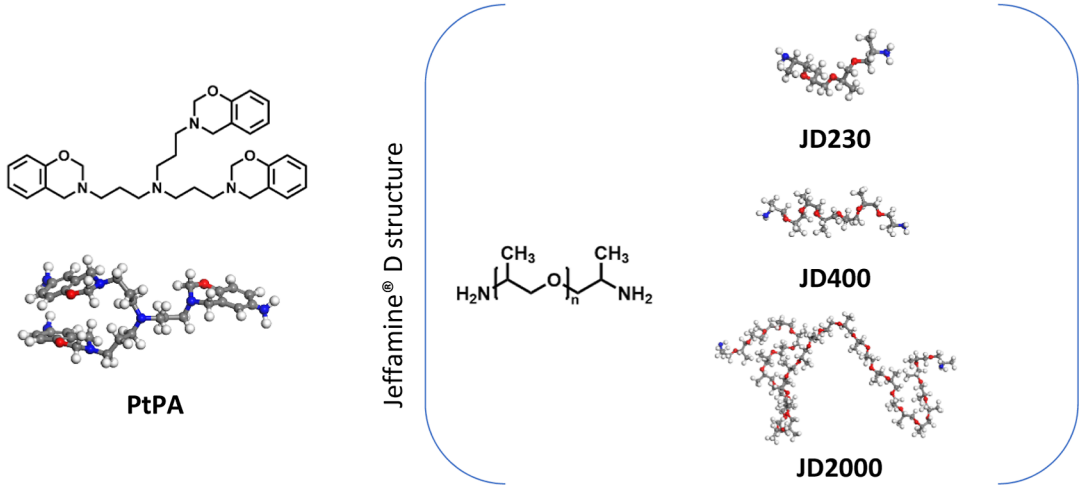


**Figure 1.** PtPA benzoxazine molecule (left) and polyetheramine (JEFFAMINES) molecules (right) investigated here.

compared with the conventional homopolymerization of benzoxazine precursors. By the choice of a suitable amine, it is possible to control and adapt the structure of the network to achieve specific properties. Along the same line, Zong and Ran[16] proved that the copolymerization between an amine and a benzoxazine can already be partially induced at room temperature depending on the solvent.

Despite these interesting features, benzoxazine chemistry has been almost exclusively dedicated to the preparation of thermoset materials with the widest possible glassy zone, leading to brittle materials. While some studies have focused on the development of benzoxazine resins with combined flexibility, ductility, and high glass transition temperature ($T_g$),[17−24] not much effort has been reported yet on the use of a benzoxazine motif to prepare elastomers.[25] In 2016, Huang et al.[26] synthesized a functional polyether-based elastomer with a benzoxazine structure in its main chain. However, the rubber characteristic of the structure was lost with the opening of the benzoxazine rings, which turns the material into a thermoset. In 2018, Advincula et al.[27] toughened a benzoxazine resin with two types of rubbers (hydroxyl-terminated and epoxidized polybutadiene) via melt mixing and chemical grafting. They found that the rubber-modified polybenzoxazine was able to protect carbon steel from corrosion. In 2021, Ishida et al.[28] have reported the development of high-char-yielding elastomers based on polydimethylsiloxane oligomers functionalized with benzoxazine groups for adhesive applications.

These few examples are far from reflecting all possibilities that could be envisioned for benzoxazine elastomers as many different industrial sectors such as transport, bio-medical, construction, electronics, and so forth make extensive use of rubbery materials and require more and more technicality. In this respect, it seems interesting to further examine the potential of benzoxazines for specific applications as elastomers due to their wide and unmatched range of properties.

The work reported here is part of a large-scale effort to develop an innovative generation of patterned coatings based on benzoxazine thermo- and photoresist matrices incorporating electrically conductive 2D layers for wide-range pressure sensing applications. Because we are particularly interested in the low-pressure regimes (<10 kPa) typical of gentle touch, there is a need to achieve low $T_g$ resins (i.e., below room temperature) and to reduce their storage modulus $E'$ down to the kPa range. For this purpose, we have designed, synthesized, and fully characterized novel elastomeric benzoxazine systems based on the copolymerization ability of benzoxazine with amines. On the one hand, a novel trifunctional benzoxazine structure based on tris(3-aminopropyl)amine and phenol reagents is synthesized. It is abbreviated PtPA and presented in Figure 1 and Scheme 1. PtPA carries three benzoxazine

**Scheme 1. Synthesis of the PtPA Trifunctional Benzoxazine**

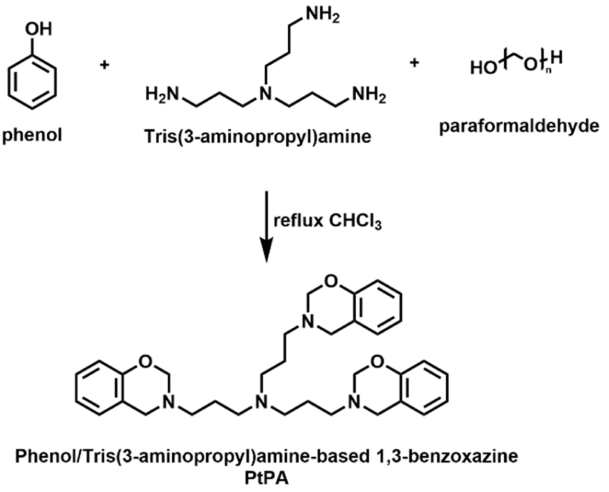


functional groups acting as cross-linking nodes (i.e., six binding sites). On the other hand, polyetheramines (JEFFAMINES), which are diamines end-substituting a propylene oxide polyether backbone, are used as soft segments between cross-links. Polyetheramines of different lengths, hereafter called JD230, JD400, and JD2000, have been selected in order to allow the modulation of the flexibility of the network[26] and thus the tuning of the thermal and mechanical properties of the resulting resins, in particular the storage modulus and $T_g$, for the targeted pressure-sensing applications.

We report below on a joint experimental modeling strategy in which dynamic mechanical and rheological measurements are compared with molecular dynamics (MD) simulations, which aims at a fundamental understanding of how the soft parts in the microstructure/network affect the topology and thermomechanical properties of the materials. MD simulations are an increasingly relevant tool in polymer science as they


https://doi.org/10.1021/acs.macromol.2c01593
Macromolecules 2022, 55, 10831−10841

provide complementary insight to experimental investigations and have reached the level of accuracy needed for a predictive assessment of the performance of new formulations. The first efforts to model the formation of polymer networks can be traced back to the 80s and were based on Monte Carlo simulations using lattice models[29] and kinetic simulations.[30] Thereafter, more sophisticated methods were developed to provide a fully atomistic description of polymer networks, such as classical force-field-based MD progressive cross-linking simulations based on distance criteria between the active centers for the construction of polymer networks.[31] This approach offers a realistic description of the polymerization process and provides access to the microstructure and the overall network topology.[32] Therefore, it has been extensively applied to the simulation of different cross-linked polymers[32−36] in order to study their thermomechanical properties.[37−41] Kim and Mattice[42−45] explored the conformational distribution of single chains and the structure of thin benzoxazine films. The analysis of the supramolecular network structures revealed the role of hydrogen bonding in the polymerization process and the properties of the polybenzoxazines.[46−50] In particular, the predicted thermomechanical properties of polybenzoxazines showed an excellent agreement with the experimental results, highlighting the ability of molecular simulations to accurately describe the properties of polybenzoxazines.[2,51−54]

## 2. EXPERIMENTAL SECTION

**2.1. Materials.** Tris(3-aminopropyl)amine (>97%) was purchased from TCI. Phenol (>99%) was obtained from Merck Millipore. Paraformaldehyde (>99%) and chloroform were used as received from VWR. Poly(propylene glycol) bis(2-aminopropyl ether) (JEFFAMINES D-230, D-400, D-2000) and magnesium sulfate (>98%) were purchased from Sigma-Aldrich.

**2.2. Preparation of Phenol/Tris(3-aminopropyl)amine-Based Benzoxazine (PtPA).** Into a 100 mL round-bottom flask were added 5 mL of chloroform per gram of reactants, phenol (2.85 g, 0.03 mol), tris(3-aminopropyl)amine (2 mL, 0.01 mol), and paraformaldehyde (1.82 g, 0.06 mol) (Scheme 1). The mixture was then stirred at reflux for 4 h. After cooling to room temperature, the reaction mixture was added with anhydrous $MgSO_4$, filtered by Büchner, and dried under vacuum to obtain PtPA as a translucent soft solid. $^1$H NMR ($CDCl_3$, ppm, $\delta$): 7.24−6.65 (m, 12H, Ar), 4.84 (s, 6H, $CH_2$ oxazine), 3.96 (s, 6H, $CH_2$ oxazine), 2.79−2.70 (t, 6H, $CH_2$ propyl), 2.48−2.42 (t, 6H, $CH_2$ propyl), 1.71−1.63 (t, 6H, $CH_2$ propyl). The full set of NMR spectra are provided in the Supporting Information (see Figures S1−S5). Fourier transform infrared (FTIR) $\nu$ ($cm^{-1}$): 1219 (asymmetric stretching of C−O−C), 1033 (symmetric stretching of C−O−C), and 922 (oxazine ring mode). Electrospray ionization mass spectrometry (ESI-MS): $C_{33}H_{42}N_4O_3$ $[M\text{-}H]^+$: $m/z$ 542.3. The ESI-MS of the product is also presented in the Supporting Information (see Figure S6).

**2.3. General Formulation of the PtPA/JEFFAMINE Copolymers.** PtPA and JEFFAMINE in the ratio of 1:1 Bz/$NH_2$ were mixed in chloroform (5 mL per gram of reactants) at room temperature, dried under vacuum to obtain a viscous liquid, and cured at 100, 120, 140, and 160 °C for 1 h at each temperature separately.

**2.4. Characterization.** 1D and 2D $^1$H and $^{13}$C NMR spectra were recorded on a Bruker AMX-500 (500 MHz) NMR spectrometer in chloroform-$d$ ($CDCl_3$) with trimethyl silane (TMS) as an internal standard. FTIR spectra were obtained using a Bruker Tensor 17 FTIR spectrometer operating in the ATR-FTIR ("attenuated total reflectance-FTIR") mode. Differential scanning calorimetry (DSC) data were obtained from a DSC 2920 apparatus (TA Instruments) at a heating rate of 10 °C $min^{-1}$ in a nitrogen flow (88 mL $min^{-1}$) for all tests. Dynamic mechanical analysis (DMA) was carried out with a DMA 850 (TA Instruments) analyzer in the parallel plate compression mode using a temperature sweep at a heating rate of 3 °C $min^{-1}$ from approximately −100 to 200 °C and a frequency of 1 Hz with an amplitude of 10 $\mu$m. The samples were 10 mm in width and roughly 6 mm thick. Rheology dynamic analysis (RDA) was performed with a MCR 302 rheometer (Anton Paar) in the parallel plate shearing mode using a strain amplitude sweep at room temperature at a frequency of 1 Hz. The samples were 25 mm in width and roughly 1 mm thick. This MCR 302 rheometer (Anton Paar) in parallel plate was also used to study the curing of the blends with a temperature sweep at 1 Hz and 0.01% strain using successive isotherms at 100, 120, 140, and 160 °C of 1 h each, except for the PtPA-JD2000, for which the isotherm at 160 °C lasted 3 h. The samples were 8 mm in width and 0.8 mm thick. ESI-MS data were acquired on a Waters Synapt G2-Si mass spectrometer (Waters, UK) equipped with an ESI source used in the positive ion mode. Samples were prepared as follows: 2 $\mu$L of a 1 mg $mL^{-1}$ THF solution was added into 1 mL of methanol to reach a final concentration of 2 × $10^{-6}$ g $mL^{-1}$. For mass spectrometer parameters, the ESI conditions were capillary voltage 3.1 kV, cone voltage 30 V, source temperature 120 °C, and desolvation temperature 150 °C. Dry nitrogen, the desolvation gas, was used as the ESI gas with a flow rate of 500 L $h^{-1}$.

**2.5. Modeling.** All simulations in this work were performed using the Materials Studio 7.0 package. The atomic interactions were described by the Dreiding force field,[55] which was optimized to reproduce at best the behavior of the studied molecules.[2] The van der Waals and electrostatic interactions were computed using the Lennard-Jones (12-6) and Coulombic potentials, respectively, with a cutoff distance of 1.2 nm. The partial charges on the atoms were computed using the Gasteiger iterative method.[56] Throughout all simulations, the pressure in *NPT* (constant number of particles, pressure, and temperature) simulations was controlled with the Parrinello−Rahman barostat at 1 atm. The temperature of the systems was controlled using the Nosé−Hoover−Langevin thermostat with a $Q$ ratio of 0.01 and the decay constant set at 1 ps.[57]

The model systems for the initial pure PtPA resin consist of 200 monomer molecules packed into 3D periodic cells at low density (0.6 g/$cm^3$). The PtPA/JEFFAMINE mixtures were prepared in a ratio of 1:1 Bz/$NH_2$. For this, 100 PtPA monomers are mixed with 150 polyetheramine chains (either JD230, JD400, or JD2000); see Figure 1. The structures are equilibrated in the *NVT* (constant number of particles, volume, and temperature) ensemble for 1 ns at 500 K, followed by an *NPT* simulation for 4 ns at 300 K, gradually leading to a dense phase.

The polymerization is modeled in a stepwise manner using the cyclic polymerization atomistic model with conducted multistep topology relaxation.[2] For the pure PtPA, we consider a ring-opening mechanism of benzoxazines by binding the monomers to each other. A distance-based criterion ranging from 0.4 to 0.9 nm is used to identify the close contacts and trigger the formation of new bonds between the reactive atoms on each monomer/chain segment. New covalent bonds between the N−C group and the ortho carbon are formed each time the distance criterion is satisfied.[58] Once all reactive sites satisfying the criterion are treated, the system undergoes a multistep relaxation-perturbation procedure using the NVT-NPT dynamics at temperatures ranging from 300 to 500 K. If the predefined conversion value is not reached, a new attempt of bond creations is then initiated. For the case of PtPA/JEFFAMINE copolymers, the reactions correspond to the bonding between the benzoxazine and polyetheramine moieties.

The structural characteristics of the network are calculated through the monitoring of the macromolecular parameters during the cross-linking: the reduced weight average degree of polymerization, which defines the gel-point,[59] and the gel fraction. For the analysis of the network topology, the MD simulations allow to disentangle the gel fraction and calculate the exact numbers of elastically active chains (giving access to the cross-link density) and also of dangling and loop chains, which represent structural defects. All molecules in the sol phase, that is, monomers and oligomers, are considered as "free chains." The structural defects, such as dangling-loop chains, and the


https://doi.org/10.1021/acs.macromol.2c01593
Macromolecules 2022, 55, 10831−10841

Table 1. Polyetheramines (JEFFAMINES) Used to Modulate the Properties of the PtPA Resins

| Commercial Name | Chain Architecture | | |
|---|---|---|---|
| JEFFAMINE® D structure | 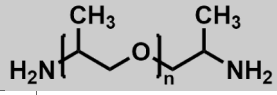 | | |
| | Code | n | Molecular Weight ($g.mol^{-1}$) |
| JEFFAMINE® D-230 | JD230 | ≅ 2.5 | 230 |
| JEFFAMINE® D-400 | JD400 | ≅ 6.1 | 430 |
| JEFFAMINE® D-2000 | JD2000 | ≅ 33 | 2000 |

elastically active chains are counted by means of a home-made algorithm described in our previous work.[2]

At several stages along the polymerization process, the reaction is stopped, and the thermomechanical properties of the cross-linked networks are assessed by a stepwise temperature excursion going from high to low temperatures to examine both the rubbery and glassy states. First, the structures are equilibrated at 700 K for 5 ns in the *NPT* ensemble and then cooled down stepwise to 50 K with a relaxation period of 2 ns between two steps. This cooling rate is sufficient for the structures to reach the equilibrium at each step. The temperature, volume, valence, and nonbonded energies are averaged and stored for further analysis. The glass transition temperature is defined as the intersection of the linear density−temperature curves of the glassy and rubbery states.

## 3. RESULTS AND DISCUSSION

**3.1. Reactivity between PtPA and JEFFAMINES.** The new trifunctional benzoxazine was synthesized according to the classical one-pot Mannich condensation from phenol, tris(3-aminopropyl)amine, and paraformaldehyde in chloroform, as shown in Scheme 1. The curing profile of the reaction between PtPA and three different JEFFAMINES from the D-serie (Table 1) was sequentially evaluated by DSC. As shown in Figure 2 and Table 2, pure PtPA displays a maximum in the

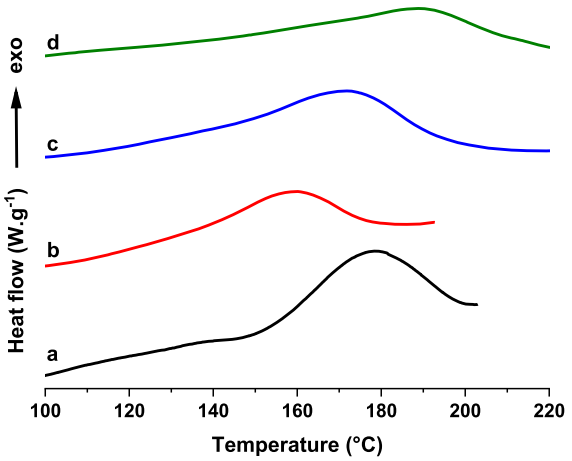


**Figure 2.** DSC thermograms of (a) pure PtPA, (b) PtPA-JD230, (c) PtPA-JD400, and (d) PtPA-JD2000. The curves have been shifted vertically for the sake of clarity.

polymerization exotherm ($T_p$) at 178 °C and an enthalpy of 182 J $g^{-1}$ (the schematic network is presented in Scheme 2a). $T_p$ is relatively low here when compared to classical and commercial benzoxazine resins based on bisphenol A and aniline ($T_p$ = 250 °C). This result can be explained by the presence of a tertiary amine on the PtPA backbone, which is known to catalyze the ring-opening polymerization. Allen and Ishida[60,61] also showed that small diamines, and more particularly ethylene diamine, possess a lower temperature of polymerization and suggested that this may be a consequence of the destabilization of the oxazine rings due to this short linkage, which would generate steric hindrance. Therefore, we think that what we observe is a combined effect of the nitrogen catalytic effect and destabilization due to the short propyl linkages. When we add a JEFFAMINE in a stoichiometric molar ratio versus benzoxazine, the exotherm starts at lower temperature and covers a larger range of temperatures. Moreover, the overall reaction enthalpy strikingly decreases. This is due to the benzoxazine−amine reaction (Scheme 2b). It was previously shown[13,14,62] that the reaction mechanism between benzoxazine and amine is complex; this can lead to multiple exotherms in the DSC thermogram, and the cross-linked network formed depends on the reactivities between these two components. Moreover, Zong and Ran[16] demonstrated that this ring-opening addition reaction can partially occur at room temperature in specific solvents. It seems therefore reasonable that our benzoxazine/polyetheramine systems react at milder temperatures than pure PtPA, which induces a broader and smaller signal in the DSC thermograms. We can also observe that (i) the longest polyetheramine yields the largest lowering in enthalpy, as illustrated by the vanishingly small exotherm in the corresponding DSC curve and (ii) JEFFAMINEs of increasing lengths induce a gradual shift of the maximum of the exotherm. We associate both results to the dilution effect.[63]

Table 2. Thermal and Rheological Properties of the Curing Systems

| curing system | molar ratio Bz/$NH_2$ | $T_p$ (°C) | $\Delta H$ (J $g^{-1}$) | complex viscosity $\eta^*$ (Pa s) |
|---|---|---|---|---|
| pure PtPA | | 178 | 182 | ≅7770 |
| PtPA-JD230 | 1:1 | 160 | 71 | ≅2725 |
| PtPA-JD400 | 1:1 | 172 | 92 | ≅2210 |
| PtPA-JD2000 | 1:1 | 189 | 22 | ≅3 |

The polymerization of the different systems was also followed by rheology during curing. As can be seen in Figure 3a,b, the increase of the complex viscosity $\eta^*$ is delayed with the length of the amine moiety due to dilution effect of the JEFFAMINE, which confirms the DSC results. Moreover, and as expected, at the end of the curing process, the longer the amine component, the smaller the complex viscosity $\eta^*$ of the resulting resin (Table 2). In particular, a value as low as 3.35


https://doi.org/10.1021/acs.macromol.2c01593
Macromolecules 2022, 55, 10831−10841

Scheme 2. Schematic Network after Polymerization of (a) Pure-PtPA and (b) PtPA-JEFFAMINE D-serie Copolymer

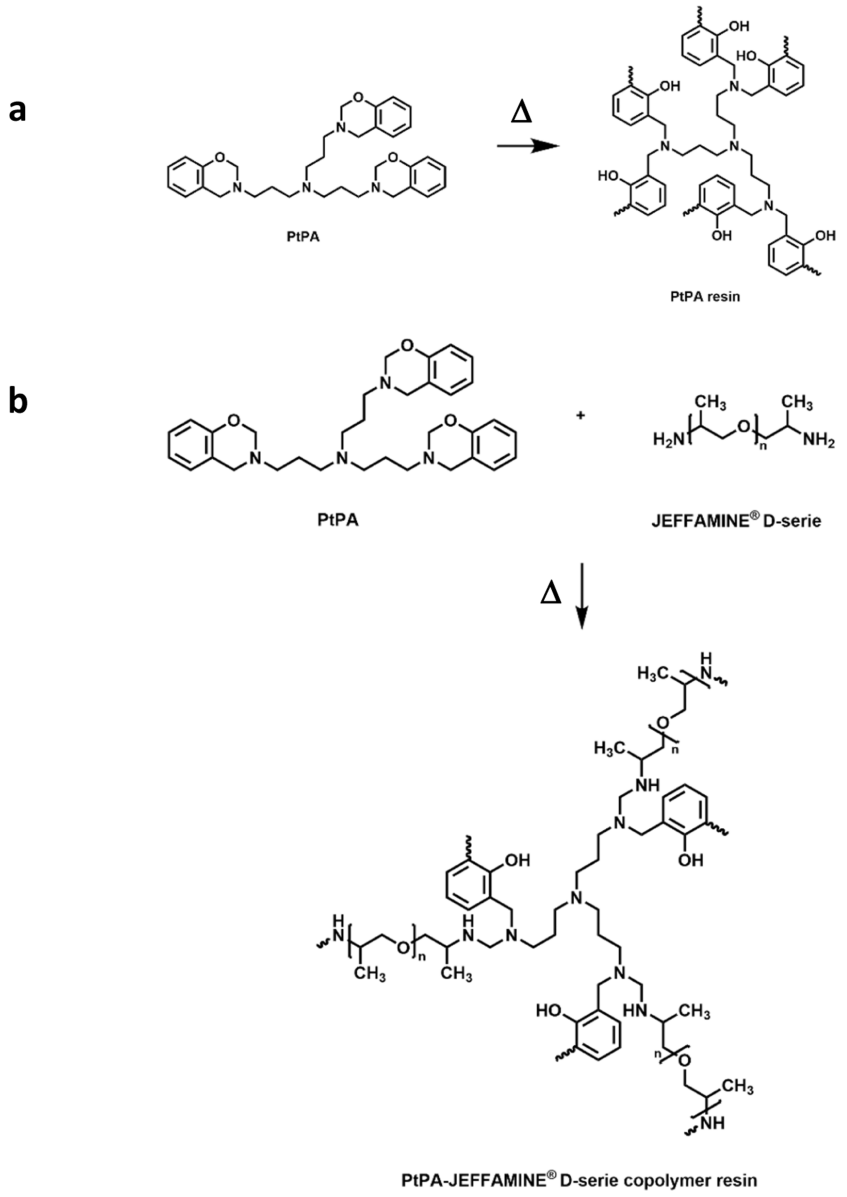


Pa s (similar to honey at room temperature) is reached for the PtPA-JD2000 resin.

After various consecutive heating stages of the blends (curing conditions: 100 °C/1 h + 120 °C/1 h + 140 °C/1 h + 160 °C/1 h, except for PtPA-JD2000 for which 3 h at 160 °C are necessary), the DSC curves no longer show a polymerization exotherm, which suggests that benzoxazine moieties are no longer present in the medium, that is, they have all reacted. To further confirm the benzoxazine ring-opening addition reaction of amine, we then analyzed the FTIR spectra of the blends before and after curing. As seen in Figure 4, the C−O−C symmetric and asymmetric stretching modes at 1033 and 1220 $cm^{-1}$, respectively, and the band at 922 $cm^{-1}$ characteristic of the oxazine ring mode[64] disappear after the curing process, which confirms the complete formation of the thermosets.

**3.2. Analysis of the Network Topology.** The structural morphology of the networks is assessed by means of MD simulations. The maxima of reduced degree of polymerization (RDP) and the gel fraction $W_g$ permit to estimate the gel point during the polymerization process. Figure 5 shows the evolution of these structural characteristics as a function of the degree of conversion. The gelation point calculated from the RDP curves is 28.7 ± 2.5, 75.1 ± 2.2, 77.6 ± 2.8, and 79.1 ± 3.2% for pure PtPA, PtPA-JD230, PtPA-JD400, and PtPA-JD2000, respectively. This is consistent with the sudden increase of $W_g$ at the gel point, which corresponds to the divergence of the largest structural molecule to an "infinite" size. The calculated values for all resins are in good agreement with the theoretical gel points determined using Flory's model of critical conversion: (i) 20% for hexafunctional molecules (pure PtPA); (ii) 71% for the stoichiometric mixtures composed of di- and trifunctional copolymers. The small discrepancy between the theoretical and simulated gel points stems from the fact that Flory's model is designed for ideal cross-linking processes and does not account for geometrical constraints and intrachain reactions.[65]

The cross-link density $\nu_e$ is extensively used for the characterization of cross-linked polymers since it can be experimentally estimated through the equilibrium modulus in


https://doi.org/10.1021/acs.macromol.2c01593
Macromolecules 2022, 55, 10831−10841

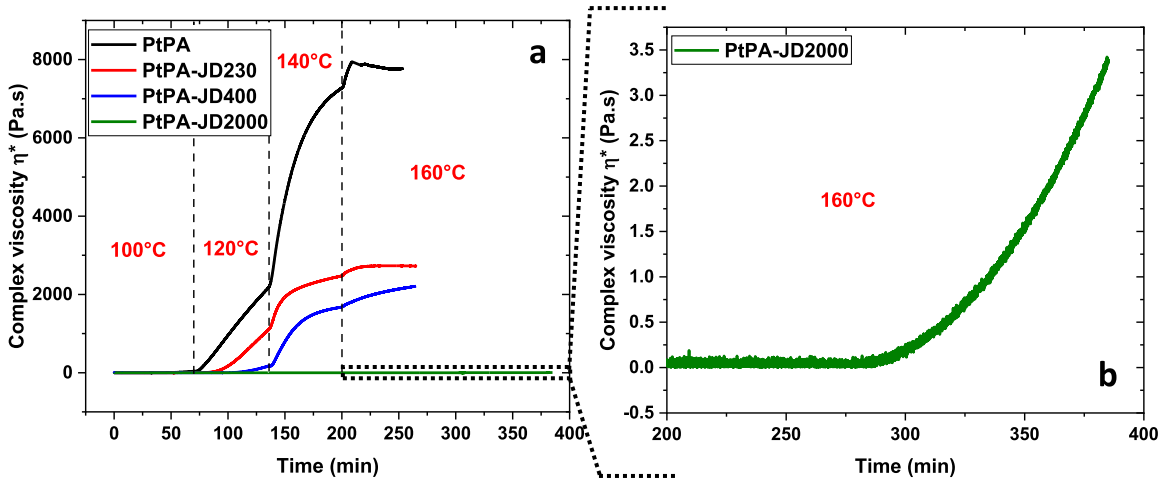


**Figure 3.** Rheology curves (temperature range: from room temperature to 160 °C) of pure PtPA, PtPA-JD230, PtPA-JD400, and PtPA-JD2000. Complex viscosity $\eta^*$ as a function of curing time and temperature (a) and vertical scale expansion between 200 and 385 min for the PtPA-JD2000 curve (b).

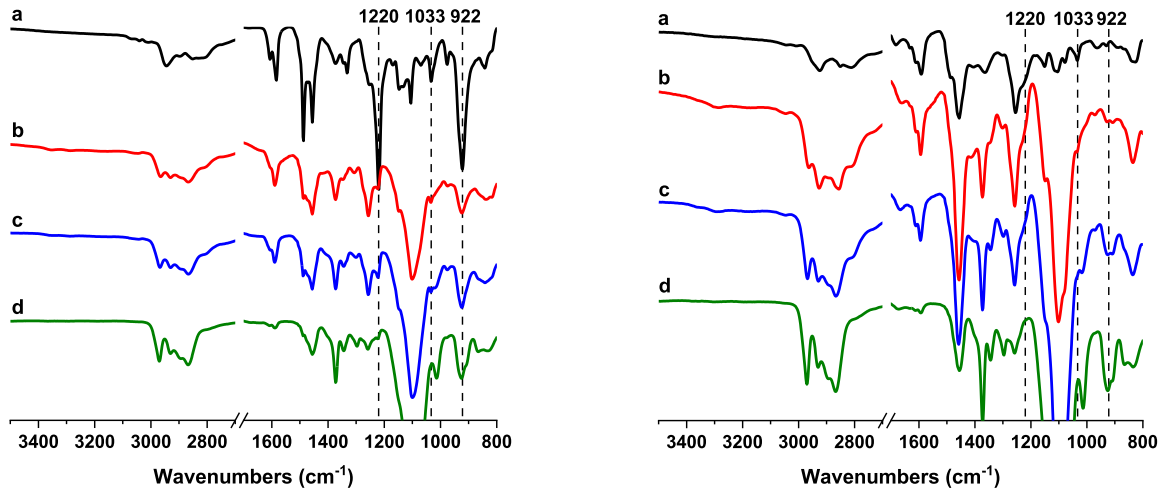


**Figure 4.** FTIR spectra of the uncured (left) and cured (right) resins of (a) pure PtPA, (b) PtPA-JD230, (c) PtPA-JD400, and (d) PtPA-JD2000. Curing conditions: 100 °C/1 h + 120 °C/1 h + 140 °C/1 h + 160 °C/1 h, except for PtPA-JD2000 for which 3 h at 160 °C are necessary.

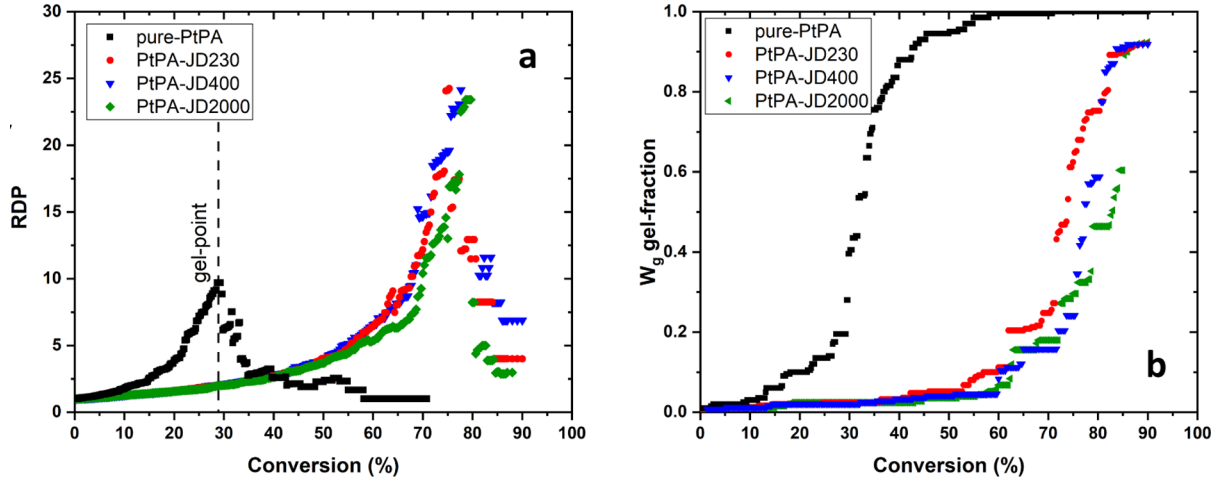


**Figure 5.** Evolution of the (a) RDP and (b) gel fraction as a function of the conversion rate for pure PtPA, PtPA-JD230, PtPA-JD400, and PtPA-JD2000.

the rubbery state.[66] However, due to the experimental limitations, the number of structural defects (dangling and loop chains) in the thermoset networks cannot be directly measured. From the MD simulations, it is possible to calculate



https://doi.org/10.1021/acs.macromol.2c01593
Macromolecules 2022, 55, 10831−10841

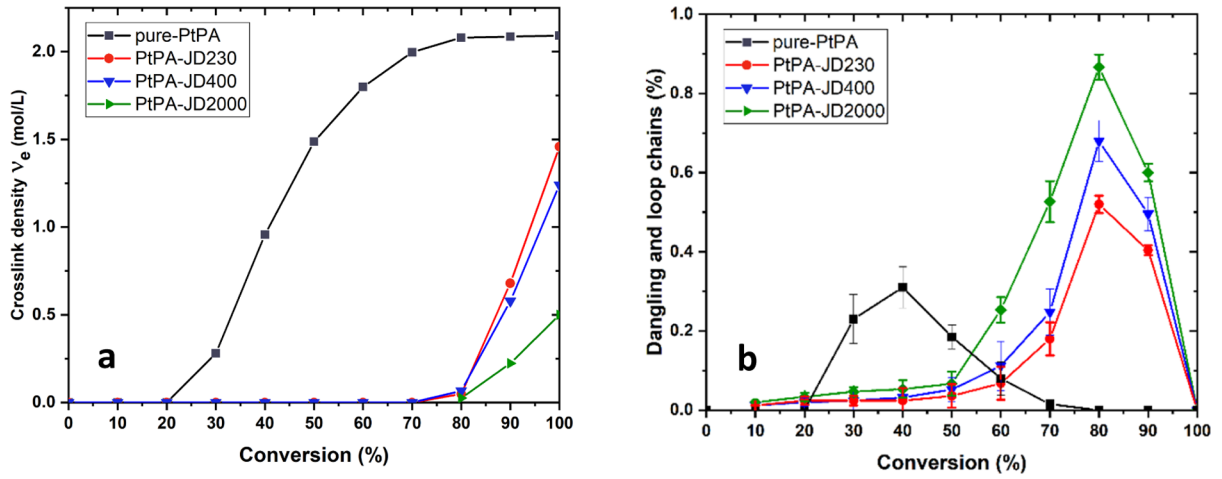


**Figure 6.** Evolution of the (a) cross-link density and (b) structural defects (dangling and loop chains) as a function of the conversion rate for pure PtPA, PtPA-JD230, PtPA-JD400, and PtPA-JD2000.

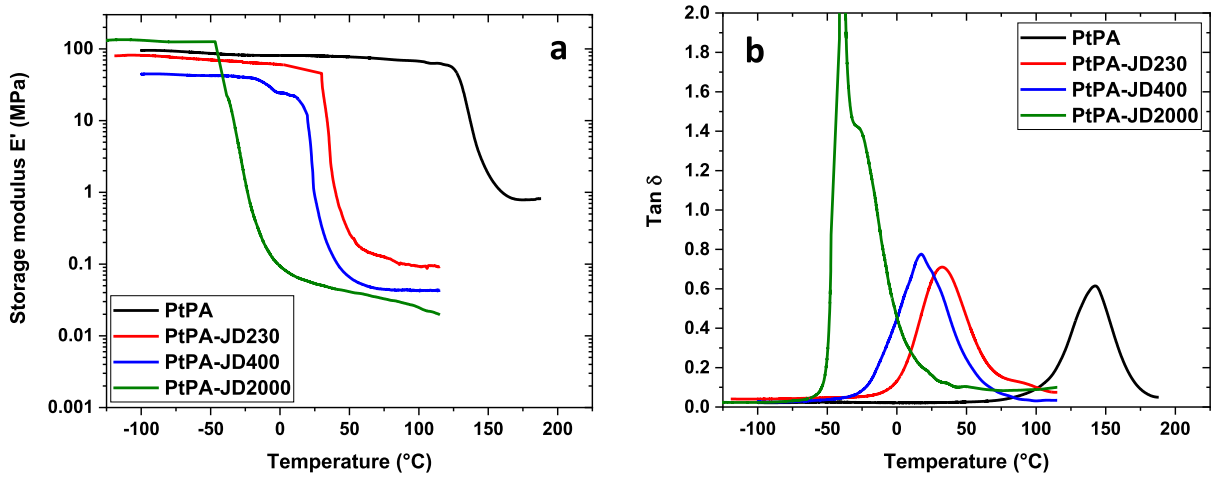


**Figure 7.** DMA thermograms (temperature sweep, frequency = 1 Hz, and ramp rate = 3 °C $min^{-1}$) of the cured pure PtPA, PtPA-JD230, PtPA-JD400, and PtPA-JD2000 resins. Storage modulus (a) and tan $\delta$ (b).

the exact value of $\nu_e$ by taking specifically the number of dangling and loop chains into account. The MD simulations offer a direct access to the number of structural chains and can therefore be used as a tool that, combined with the experimental results, can feed experimental prediction models.[32]

Figure 6a,b depicts the evolution of the cross-link density $\nu_e$ and the number of structural defects (dangling and loop chains) versus the degree of conversion. The appearance of the first elastic chains in the pure PtPA and PtPA-JEFFAMINES structures is consistent with the calculated gel points. For the fully cross-linked networks, the cross-link density is 2.1 mol $L^{-1}$ for pure PtPA. As expected, due to the larger size of the PtPA precursor, this value is lower than in previously studied tetrafunctional polybenzoxazines,[2] where $\nu_e$ ranges from 2.5 to 3.6 mol $L^{-1}$, since for fully polymerized structures, each cross-link originates from one monomer. The cross-link density is much lower for the PtPA-JEFFAMINES systems due to the presence of polypropylene oxide segments of increasing length: 0.68, 0.57, and 0.22 mol $L^{-1}$ for JD230, JD400, and JD2000, respectively. This lower cross-link density is expected to manifest in the decrease of the elastic and thermomechanical properties of these resins and is indeed observed; see below. The number of structural defects, that is, dangling and loop chains, peaks in the region of the gel point for all polybenzoxazines. As the cross-linking proceeds beyond the gel point, the number of elastic chains increases by consuming dangling, loop, and free chains until the structures become completely elastic.

**3.3. Thermomechanical Properties of the Copolymer Resins.** We next probed the thermomechanical response of the copolymer resins by a temperature sweep in order to assess the modulation of the flexibility and elasticity of the network by the addition of the amine component to the benzoxazine reagent. Because the resins as-formed from the blends are too soft to be analyzed by DMA in the film tension mode, it was decided to examine those thermosets in the compression mode, which is more suitable for low-modulus materials like gels.[67] The curves obtained for the cured resins are shown in Figure 7 and important data extracted from the curves are summarized in Table 3. The inspection of the storage modulus data on Figure 7a shows that the value in the rubbery plateau region above $T_g$, which is proportional to the number of cross-links,[68] decreases with the backbone length of the amine compound. This is confirmed by the evolution of the tan $\delta$ height in Figure 7b, which is related to the cross-link density,


https://doi.org/10.1021/acs.macromol.2c01593
Macromolecules 2022, 55, 10831−10841

**Table 3. Thermomechanical Properties of the Cured Systems**

| curing system | storage modulus $E'$ at room temperature (MPa) | $T_g$ (°C) from tan $\delta$ | $T_g$ (°C) from onset $E'$ |
|---|---|---|---|
| pure PtPA | 80 | 143 | 127 |
| PtPA-JD230 | 45 | 32 | 29 |
| PtPA-JD400 | 0.8 | 18 | 19 |
| PtPA-JD2000 | 0.05 | −41 | −44 |

and hence, the larger the molecular weight of the amine reagent, the lower the cross-link density. From the data collected in Table 3, a trend can be identified: the ring-opening addition reaction of PtPA by means of JEFFAMINES makes it possible to tune the room-temperature storage modulus of the resins over 3 orders of magnitude. More strikingly, the glass transition temperature $T_g$, which can be taken as $T_\alpha$ from the tan $\delta$ curve or estimated from the onset of the storage modulus $E'$ curve, is dramatically reduced by the copolymerization. The decrease with respect to the pure benzoxazine markedly exceeds 100 °C, with a $T_g$ value well below room temperature for PtPA-JD2000.

Parallel to the experiments, the glass transition temperature $T_g$ of the polybenzoxazines was calculated using MD simulations by following the density of the simulated structures as a function of the temperature. Figure 8a depicts the variation with conversion of the $T_g$ for the pure PtPA resin. Up to 60% of conversion, the $T_g$ steadily increases as the gel builds up and the structural defects disappear. Thenceforth, the cross-link density gradually converges to its maximum value and $T_g$ grows at a slower pace, reaching 108 °C at 90% of conversion. This result is in reasonable agreement with the experimental result (127 °C) for the fully cured resin (estimated from the onset of the storage modulus $E'$). The $T_g$ was also determined for the PtPA-JEFFAMINES structures (Figure 8b). Again, the theoretical predictions are close to the experimental values: 34 $°C_{sim}$ versus 29 $°C_{exp}$ for PtPA-JD230, 21 $°C_{sim}$ versus 19 $°C_{exp}$ for PtPA-JD400, and −8 $°C_{sim}$ versus −44 $°C_{exp}$ for PtPA-JD2000. It can be seen that the thermomechanical properties of the polybenzoxazine blends strongly depend on the size of the JEFFAMINE chain extenders and are intimately related to the cross-link density of the resins.

In addition to the thermomechanical characterization of the samples by DMA in the compression mode, we tested the systems by RDA in the oscillatory shear mode (Figure 9). We performed a strain amplitude sweep test at room temperature and 1 Hz. These experiments make it possible to determine the shear resistance of the materials at room temperature. The storage modulus $G'$ of all systems is higher than the loss modulus $G''$ and remains constant at low shear strain, confirming that the materials are cross-linked and exhibit solidlike behavior. In addition, the room-temperature value of $G'$ at the zero-strain limit is found to decrease strongly (about 2−3 decades) with the length of the polyetheramine, except for JD230. This can be explained by the fact that the PtPA-JD400 and PtPA-JD2000 systems are elastomers at room temperature, whereas the pure PtPA and PtPA-JD230 resins are glassy materials at room temperature. $G'$ in the elastomeric systems (i.e., PtPA-JD400 and PtPA-JD2000) remains constant over

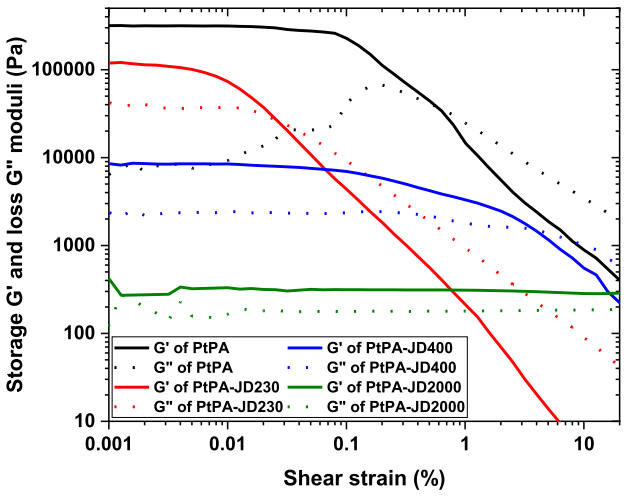


**Figure 9.** RDA curves (amplitude sweep, frequency = 1 Hz at room temperature) of the cured resins of pure PtPA, PtPA-JD230, PtPA-JD400, and PtPA-JD2000.

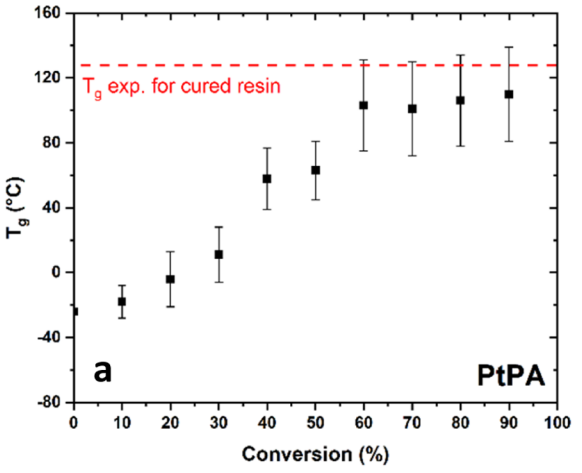


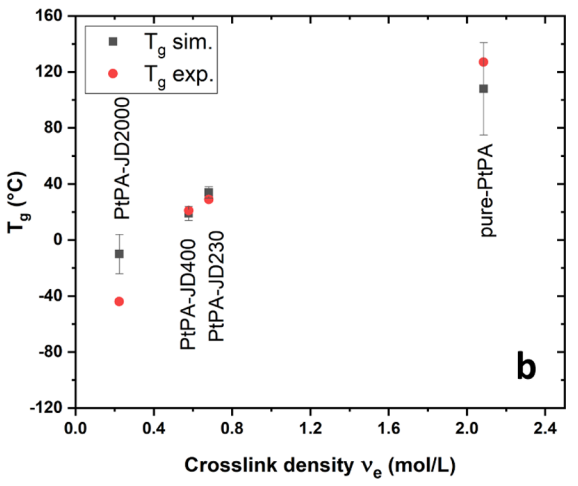


**Figure 8.** (a) Glass transition temperature with conversion degree calculated from MD simulations for the pure PtPA resin. (b) Relationship between the calculated cross-link density and the calculated (red symbols) and measured (black symbols) glass transition temperature for the fully cured structures for pure PtPA, PtPA-JD230, PtPA-JD400, and PtPA-JD2000.



https://doi.org/10.1021/acs.macromol.2c01593
Macromolecules 2022, 55, 10831−10841

the larger range of shear strain, highlighting the fact that for long polyether chains, the low cross-link density of the network turns into softer materials that can withstand larger deformation.

Overall, the thermomechanical data in compression (as obtained by DMA) and under shear (as obtained by RDA) clearly confirm that the longer the JEFFAMINE backbone, the better the copolymer resin elasticity and flexibility.

## 4. CONCLUSIONS

In this work, a novel trifunctional benzoxazine precursor based on tris(3-aminopropyl)amine and phenol reagents (PtPA) was successfully synthesized. Due to the presence of a tertiary amine in the backbone of PtPA, its thermal homopolymerization takes place at a relative low temperature (178 °C) when compared to classical and commercial benzoxazine resins based on bisphenol A and aniline (250 °C).

The resulting material is a thermoset presenting a $T_g$ of about 143 °C, a compression modulus of about 80 MPa, as determined by DMA at room temperature, a shear modulus of about 3 GPa, and a shear strain resistance lower than 0.5%, as determined by RDA at room temperature.

With the aim of designing elastic resins for soft pressure sensing, we next copolymerized PtPA with polyetheramines of different lengths (JD230 = 230 g mol$^{-1}$, JD400 = 400 g mol$^{-1}$, and JD2000 = 2000 g mol$^{-1}$), finding a drastic decrease in the cross-link density. This is especially the case for JD2000 and JD400, which behave as elastomeric materials.

More generally, the longer the polyether chain, the lower the $T_g$ (−41 °C for JD2000), the lower the modulus in compression (50 kPa for JD2000), the lower the shear modulus (about 300 Pa for JD2000), the higher the shear strain resistance (higher than 10% for JD2000), and ultimately the softer the resins. These experimental results are backed-up by advanced modeling investigations providing a clear link between the cross-linking density and the $T_g$ of the resins.

These results highlight the high efficiency of the copolymerization approach to adjust the cross-linking density of the benzoxazine network in order to develop materials with suitable thermomechanical properties for sensing applications.

## ■ ASSOCIATED CONTENT

### Supporting Information

The Supporting Information is available free of charge at https://pubs.acs.org/doi/10.1021/acs.macromol.2c01593.

1D and 2D $^1$H and $^{13}$C NMR spectra of PtPA benzoxazine and ESI-MS spectrum of PtPA benzoxazine (PDF)

## ■ AUTHOR INFORMATION


### Corresponding Authors

**Hugo Puozzo** − *Laboratory for Chemistry of Novel Materials, Center of Innovation and Research in MAterials & Polymers (CIRMAP) and Laboratory of Polymeric and Composite Materials (LPCM), Center of Innovation and Research in MAterials & Polymers (CIRMAP), Materia Nova Research Center, Materials Research Institute, University of Mons (UMONS), B-7000 Mons, Belgium;* orcid.org/0000-0002-0700-8449; Email: Hugo.PUOZZO@umons.ac.be

**David Beljonne** − *Laboratory for Chemistry of Novel Materials, Center of Innovation and Research in MAterials & Polymers (CIRMAP), University of Mons (UMONS), B-7000 Mons, Belgium;* orcid.org/0000-0002-2989-3557; Email: david.beljonne@umons.ac.be

### Authors

**Shamil Saiev** − *Laboratory for Chemistry of Novel Materials, Center of Innovation and Research in MAterials & Polymers (CIRMAP), University of Mons (UMONS), B-7000 Mons, Belgium*

**Leïla Bonnaud** − *Laboratory of Polymeric and Composite Materials (LPCM), Center of Innovation and Research in MAterials & Polymers (CIRMAP), Materia Nova Research Center, Materials Research Institute, University of Mons (UMONS), B-7000 Mons, Belgium*

**Julien De Winter** − *Organic Synthesis and Mass Spectrometry Laboratory (S$^2$MOs), Interdisciplinary Center for Mass Spectrometry (CISMa), University of Mons (UMONS), B-7000 Mons, Belgium;* orcid.org/0000-0003-3429-5911

**Roberto Lazzaroni** − *Laboratory for Chemistry of Novel Materials, Center of Innovation and Research in MAterials & Polymers (CIRMAP), University of Mons (UMONS), B-7000 Mons, Belgium;* orcid.org/0000-0002-6334-4068

Complete contact information is available at: https://pubs.acs.org/10.1021/acs.macromol.2c01593


### Notes

The authors declare no competing financial interest.

## ■ ACKNOWLEDGMENTS

The authors wish to thank the Fonds National de la Recherche Scientifique (FNRS) through the FLAG-ERA project PROSPECT. L.B. wishes to thank the Walloon Region and the European Commission for general support in the frame of the INTERREG V program FWVL (ATHENS project). The authors also want to thank Soumaya Lafqir and Tim Schouw for the design of the DMA sample molds. The molecular modeling activities are supported by FNRS (Consortium des Équipements de Calcul Intensif—CÉCI, under grant 2.5020.11) and by the Walloon Region (ZENOBE Tier-1 supercomputer, under grant 1117545). DB is a FNRS Research Director.

## ■ REFERENCES


(1) Ning, X.; Ishida, H. Phenolic Materials via Ring-Opening Polymerization: Synthesis and Characterization of Bisphenol-A Based Benzoxazines and Their Polymers. *J. Polym. Sci., Part A: Polym. Chem.* **1994**, *32*, 1121−1129.

(2) Saiev, S.; Bonnaud, L.; Dubois, P.; Beljonne, D.; Lazzaroni, R. Modeling the Formation and Thermomechanical Properties of Polybenzoxazine Thermosets. *Polym. Chem.* **2017**, *8*, 5988−5999.

(3) Ishida, H. Chapter 1 - Overview and Historical Background of Polybenzoxazine Research. In *Handbook of Benzoxazine Resins*; Ishida, H., Agag, T., Eds.; Elsevier: Amsterdam, 2011; pp 3−81.

(4) Ghosh, N. N.; Kiskan, B.; Yagci, Y. Polybenzoxazines—New High Performance Thermosetting Resins: Synthesis and Properties. *Prog. Polym. Sci.* **2007**, *32*, 1344−1391.

(5) Yagci, Y.; Kiskan, B.; Ghosh, N. N. Recent Advancement on Polybenzoxazine—A Newly Developed High Performance Thermoset. *J. Polym. Sci., Part A: Polym. Chem.* **2009**, *47*, 5565−5576.

(6) Kiskan, B.; Ghosh, N. N.; Yagci, Y. Polybenzoxazine-Based Composites as High-Performance Materials. *Polym. Int.* **2011**, *60*, 167−177.

(7) Arslan, M.; Kiskan, B.; Yagci, Y. Polybenzoxazines. *Encycl. Polym. Sci. Technol.* **2015**, *15*, 1−23.

(8) Dumas, L.; Bonnaud, L.; Olivier, M.; Poorteman, M.; Dubois, P. Chavicol Benzoxazine: Ultrahigh Tg Biobased Thermoset with Tunable Extended Network. *Eur. Polym. J.* **2016**, *81*, 337−346.
(9) Dumas, L.; Bonnaud, L.; Olivier, M.; Poorteman, M.; Dubois, P. High Performance Bio-Based Benzoxazine Networks from Resorcinol and Hydroquinone. *Eur. Polym. J.* **2016**, *75*, 486−494.
(10) Bonnaud, L.; Chollet, B.; Dumas, L.; Peru, A. A. M.; Flourat, A. L.; Allais, F.; Dubois, P. High-Performance Bio-Based Benzoxazines from Enzymatic Synthesis of Diphenols. *Macromol. Chem. Phys.* **2019**, *220*, 1800312.
(11) Dumas, L.; Bonnaud, L.; Olivier, M.; Poorteman, M.; Dubois, P. Facile Preparation of a Novel High Performance Benzoxazine−CNT Based Nano-Hybrid Network Exhibiting Outstanding Thermo-Mechanical Properties. *Chem. Commun.* **2013**, *49*, 9543−9545.
(12) Ohashi, S.; Ishida, H. Chapter 1 - Various Synthetic Methods of Benzoxazine Monomers. In *Advanced and Emerging Polybenzoxazine Science and Technology*; Ishida, H., Froimowicz, P., Eds.; Elsevier: Amsterdam, 2017; pp 3−8.
(13) Xu, Y.; Wang, J.; Fu, F.; Liu, X. Copolymerization and Phase Separation Behaviors of Benzoxazine−Amine Thermosets. *RSC Adv.* **2016**, *6*, 100590−100597.
(14) Sun, J.; Wei, W.; Xu, Y.; Qu, J.; Liu, X.; Endo, T. A Curing System of Benzoxazine with Amine: Reactivity, Reaction Mechanism and Material Properties. *RSC Adv.* **2015**, *5*, 19048−19057.
(15) Agag, T.; Arza, C. R.; Maurer, F. H. J.; Ishida, H. Primary Amine-Functional Benzoxazine Monomers and Their Use for Amide-Containing Monomeric Benzoxazines. *Macromolecules* **2010**, *43*, 2748−2758.
(16) Zong, J.; Ran, Q. Ring Opening Reaction of 3,4-Dihydro-2H-1,3-Benzoxazine with Amines at Room Temperature. *ChemistrySelect* **2019**, *4*, 6687−6696.
(17) Kiskan, B.; Yagci, Y.; Ishida, H. Synthesis, Characterization, and Properties of New Thermally Curable Polyetheresters Containing Benzoxazine Moieties in the Main Chain. *J. Polym. Sci., Part A: Polym. Chem.* **2008**, *46*, 414−420.
(18) Agag, T.; Geiger, S.; Alhassan, S. M.; Qutubuddin, S.; Ishida, H. Low-Viscosity Polyether-Based Main-Chain Benzoxazine Polymers: Precursors for Flexible Thermosetting Polymers. *Macromolecules* **2010**, *43*, 7122−7127.
(19) Baqar, M.; Agag, T.; Ishida, H.; Qutubuddin, S. Poly(Benzoxazine-Co-Urethane)s: A New Concept for Phenolic/Urethane Copolymers via One-Pot Method. *Polymer* **2011**, *52*, 307−317.
(20) Song, J.; Lee, J.; Kim, H. A Study on the Thermal Properties of Polyetheramine Modified Polybenzoxazines. *Macromol. Res.* **2014**, *22*, 179−186.
(21) Liu, Y.; Huang, J.; Su, X.; Han, M.; Li, H.; Run, M.; Song, H.; Wu, Y. Shape Memory Polybenzoxazines Based on Polyetheramine. *React. Funct. Polym.* **2016**, *102*, 62−69.
(22) Khan, M. M.; Halder, K.; Shishatskiy, S.; Filiz, V. Synthesis and Crosslinking of Polyether-Based Main Chain Benzoxazine Polymers and Their Gas Separation Performance. *Polymers* **2018**, *10*, 221.
(23) Li, C.; Shen, S.; Li, Z.; Zhen, H.; Huang, J.; Liu, Y. Dynamic Mechanical and Shape Memory Properties of Copolymers Based on Polyetheramine-Type Benzoxazines and Diglycidylether of Bisphenol-A. *J. Appl. Polym. Sci.* **2018**, *135*, 46838.
(24) Zhang, S.; Peng, Y.; Xue, W.; Shen, S.; Li, C.; Li, Z.; Liu, Y. Synthesis, Dynamic Mechanical Properties, and Shape Memory Effect of Polybenzoxazines Based on Monofluorophenol Isomers and Polyetheramines. *Polymer* **2019**, *166*, 169−177.
(25) Elias, H. *Macromolecules. Physical Structures and Properties*, 1st ed.; Wiley, 2008; Vol. *3*.
(26) Wan, L.; Han, D.; Liu, Q.; Xu, Z.; Huang, F. Polyether-Based Main-Chain-Type Polytriazole Elastomer with Benzoxazine via a 1,3-Dipolar Cycloaddition Reaction. *J. Appl. Polym. Sci.* **2016**, *133*, 42820.
(27) Caldona, E. B.; de Leon, A. C. C.; Mangadlao, J. D.; Lim, K. J. A.; Pajarito, B. B.; Advincula, R. C. On the Enhanced Corrosion Resistance of Elastomer-Modified Polybenzoxazine/Graphene Oxide Nanocomposite Coatings. *React. Funct. Polym.* **2018**, *123*, 10−19.
(28) Machado, I.; Rachita, E.; Fuller, E.; Calado, V. M. A.; Ishida, H. Very High-Char-Yielding Elastomers Based on the Copolymers of a Catechol/Furfurylamine Benzoxazine and Polydimethylsiloxane Oligomers. *ACS Sustainable Chem. Eng.* **2021**, *9*, 16637−16650.
(29) Sotta, P.; Higgs, P. G.; Depner, M.; Deloche, B. Monte Carlo Simulations of the Orientational Order in a Strained Polymer Network: Effect of Density. *Macromolecules* **1995**, *28*, 7208−7214.
(30) Šomvársky, J.; Dušek, K. Kinetic Monte-Carlo Simulation of Network Formation. *Polym. Bull.* **1994**, *33*, 369−376.
(31) Doherty, D. C.; Holmes, B. N.; Leung, P.; Ross, R. B. Polymerization Molecular Dynamics Simulations. I. Cross-Linked Atomistic Models for Poly(Methacrylate) Networks. *Comput. Theor. Polym. Sci.* **1998**, *8*, 169−178.
(32) Li, C.; Strachan, A. Evolution of Network Topology of Bifunctional Epoxy Thermosets during Cure and Its Relationship to Thermo-Mechanical Properties: A Molecular Dynamics Study. *Polymer* **2015**, *75*, 151−160.
(33) Li, C.; Strachan, A. Molecular Simulations of Crosslinking Process of Thermosetting Polymers. *Polymer* **2010**, *51*, 6058−6070.
(34) Wan Hassan, W. A.; Liu, J.; Howlin, B. J.; Ishida, H.; Hamerton, I. Examining the Influence of Bisphenol A on the Polymerisation and Network Properties of an Aromatic Benzoxazine. *Polymer* **2016**, *88*, 52−62.
(35) Gou, J.; Minaie, B.; Wang, B.; Liang, Z.; Zhang, C. Computational and Experimental Study of Interfacial Bonding of Single-Walled Nanotube Reinforced Composites. *Comput. Mater. Sci.* **2004**, *31*, 225−236.
(36) Li, C.; Strachan, A. Molecular Dynamics Predictions of Thermal and Mechanical Properties of Thermoset Polymer EPON862/DETDA. *Polymer* **2011**, *52*, 2920−2928.
(37) Bermejo, J. S.; Ugarte, C. M. Chemical Crosslinking of PVA and Prediction of Material Properties by Means of Fully Atomistic MD Simulations. *Macromol. Theory Simul.* **2009**, *18*, 259−267.
(38) Fan, H. B.; Yuen, M. M. F. Material Properties of the Cross-Linked Epoxy Resin Compound Predicted by Molecular Dynamics Simulation. *Polymer* **2007**, *48*, 2174−2178.
(39) Yang, S.; Qu, J. Computing Thermomechanical Properties of Crosslinked Epoxy by Molecular Dynamic Simulations. *Polymer* **2012**, *53*, 4806−4817.
(40) Sirk, T. W.; Khare, K. S.; Karim, M.; Lenhart, J. L.; Andzelm, J. W.; McKenna, G. B.; Khare, R. High Strain Rate Mechanical Properties of a Cross-Linked Epoxy across the Glass Transition. *Polymer* **2013**, *54*, 7048−7057.
(41) Bandyopadhyay, A.; Valavala, P. K.; Clancy, T. C.; Wise, K. E.; Odegard, G. M. Molecular Modeling of Crosslinked Epoxy Polymers: The Effect of Crosslink Density on Thermomechanical Properties. *Polymer* **2011**, *52*, 2445−2452.
(42) Kim, W.-K.; Mattice, W. L. A Fully Atomistic Model of an Amorphous Polybenzoxazine at Bulk Density. *Comput. Theor. Polym. Sci.* **1998**, *8*, 353−361.
(43) Kim, W.-K.; Mattice, W. L. Conformational Statistics of a Polybenzoxazine. *Comput. Theor. Polym. Sci.* **1998**, *8*, 339−351.
(44) Kim, W.-K.; Mattice, W. L. Molecular Modeling of a Thin Film of Polybenzoxazine. *Langmuir* **1998**, *14*, 6588−6593.
(45) Kim, W.-K.; Mattice, W. L. Static and Dynamic Behavior of H2O and O2 Penetrants in a Polybenzoxazine. *Macromolecules* **1998**, *31*, 9337−9344.
(46) Liu, X.; Gu, Y. Molecular Modeling of the Chain Structures of Polybenzoxazines. *Chem. Res. Chin. Univ.* **2002**, *18*, 367−369.
(47) Hall, S. A.; Hamerton, I.; Howlin, B. J.; Mitchell, A. L. Validating Software and Force Fields for Predicting the Mechanical and Physical Properties of Poly(Bisbenzoxazine)S. *Mol. Simul.* **2008**, *34*, 1259−1266.
(48) Goward, G. R.; Sebastiani, D.; Schnell, I.; Spiess, H. W.; Kim, H.-D.; Ishida, H. Benzoxazine Oligomers: Evidence for a Helical Structure from Solid-State NMR Spectroscopy and DFT-Based Dynamics and Chemical Shift Calculations. *J. Am. Chem. Soc.* **2003**, *125*, 5792−5800.


https://doi.org/10.1021/acs.macromol.2c01593
*Macromolecules* 2022, 55, 10831−10841

(49) Shen, X.; Cao, L.; Liu, Y.; Dai, J.; Liu, X.; Zhu, J.; Du, S. How Does the Hydrogen Bonding Interaction Influence the Properties of Polybenzoxazine? An Experimental Study Combined with Computer Simulation. *Macromolecules* **2018**, *51*, 4782−4799.
(50) Zhang, K.; Han, L.; Nie, Y.; Szigeti, M. L.; Ishida, H. Examining the Effect of Hydroxyl Groups on the Thermal Properties of Polybenzoxazines: Using Molecular Design and Monte Carlo Simulation. *RSC Adv.* **2018**, *8*, 18038−18050.
(51) Hamerton, I.; Howlin, B. J.; Mitchell, A. L. Developing Poly(Bis-Benzoxazines) with Improved Fracture Toughness. 1: Using Molecular Simulation to Determine and Predict Structure−Property Relationships. *React. Funct. Polym.* **2006**, *66*, 21−39.
(52) Hamerton, I.; Howlin, B. J.; Mitchell, A. L.; Hall, S. A.; McNamara, L. Chapter 5 - Using Molecular Simulation to Predict the Physical and Mechanical Properties of Polybenzoxazines. In *Handbook of Benzoxazine Resins*; Ishida, H., Agag, T., Eds.; Elsevier: Amsterdam, 2011; pp 127−142.
(53) Wan Hassan, W. A.; Hamerton, I.; Howlin, B. J. Prediction of Selected Physical and Mechanical Properties of a Telechelic Polybenzoxazine by Molecular Simulation. *PLoS One* **2013**, *8*, No. e61179.
(54) Thompson, S.; Stone, C. A.; Howlin, B. J.; Hamerton, I. Exploring Structure−Property Relationships in Aromatic Polybenzoxazines Through Molecular Simulation. *Polymers* **2018**, *10*, 1250.
(55) Mayo, S. L.; Olafson, B. D.; Goddard, W. A. DREIDING: A Generic Force Field for Molecular Simulations. *J. Phys. Chem.* **1990**, *94*, 8897−8909.
(56) Gasteiger, J.; Marsili, M. Iterative Partial Equalization of Orbital Electronegativity—a Rapid Access to Atomic Charges. *Tetrahedron* **1980**, *36*, 3219−3228.
(57) Samoletov, A. A.; Dettmann, C. P.; Chaplain, M. A. J. Thermostats for "Slow" Configurational Modes. *J. Stat. Phys.* **2007**, *128*, 1321−1336.
(58) Ishida, H.; Sanders, D. P. Regioselectivity of the Ring-Opening Polymerization of Monofunctional Alkyl-Substituted Aromatic Amine-Based Benzoxazines. *Polymer* **2001**, *42*, 3115−3125.
(59) Shy, L. Y.; Leung, Y. K.; Eichinger, B. E. Critical Exponents for Off-Lattice Gelation of Polymer Chains. *Macromolecules* **1985**, *18*, 983−986.
(60) Allen, D. J.; Ishida, H. Effect of Phenol Substitution on the Network Structure and Properties of Linear Aliphatic Diamine-Based Benzoxazines. *Polymer* **2009**, *50*, 613−626.
(61) Allen, D. J.; Ishida, H. Polymerization of Linear Aliphatic Diamine-Based Benzoxazine Resins under Inert and Oxidative Environments. *Polymer* **2007**, *48*, 6763−6772.
(62) Zhao, Y.; Xu, Y.; Xu, Q.; Fu, F.; Zhang, Y.; Endo, T.; Liu, X. Significant Improvement on Polybenzoxazine Toughness Achieved by Amine/Benzoxazine Copolymerization-Induced Phase Separation. *Macromol. Chem. Phys.* **2018**, *219*, 1700517.
(63) Shukla, S.; Lochab, B. Role of Higher Aromatic Content in Modulating Properties of Cardanol Based Benzoxazines. *Polymer* **2016**, *99*, 684−694.
(64) Han, L.; Iguchi, D.; Gil, P.; Heyl, T. R.; Sedwick, V. M.; Arza, C. R.; Ohashi, S.; Lacks, D. J.; Ishida, H. Oxazine Ring-Related Vibrational Modes of Benzoxazine Monomers Using Fully Aromatically Substituted, Deuterated, 15N Isotope Exchanged, and Oxazine-Ring-Substituted Compounds and Theoretical Calculations. *J. Phys. Chem. A* **2017**, *121*, 6269−6282.
(65) Flory, P. J. Molecular Size Distribution in Three Dimensional Polymers. I. Gelation1. *J. Am. Chem. Soc.* **1941**, *63*, 3083−3090.
(66) Flory, P. J. Molecular Theory of Rubber Elasticity. *Polymer* **1979**, *20*, 1317−1320.
(67) TA Instruments. *Discovery DMA Brochure*, 2018.
(68) Menard, K. P.; Menard, N. R. *Dynamic Mechanical Analysis*, 3rd ed.; CRC Press, 2020; Vol. *148*.





https://doi.org/10.1021/acs.macromol.2c01593
*Macromolecules* 2022, 55, 10831−10841